GROUND-BASED GEOPHYSICAL INVESTIGATIONS IN THE SECO CREEK AREA, MEDINA COUNTY, TEXAS

by

Jeffrey G. Paine and Edward W. Collins
Bureau of Economic Geology
John A. and Katherine G. Jackson School of Geosciences
The University of Texas at Austin

Mail address:
University Station, Box X
Austin, Texas 78713-8924

Street address:
J. J. Pickle Research Campus, Building 130
10100 Burnet Road
Austin, Texas 78758-4445
jeff.paine@beg.utexas.edu

Report prepared for

U.S. Geological Survey
P. O. Box 25046, MS 973
Denver Federal Center
Denver, Colorado 80225

Order No. 02CRSA0768

November 2003

Page intentionally blank

CONTENTS

FIGURES

SUMMARY

In May 2003, we acquired ground conductivity measurments at 379 locations along nine lines on and near Seco Creek, Medina County, Texas, in support of an airborne geophysical survey flown for the U.S. Geological Survey in 2002. These measurements, made using a ground-based instrument, demonstrate that (a) mapped geologic units consisting of Cretaceous limestones and dolomitized limestones, marls, mudstones, and shales and Quaternary alluvial deposits have mappable differences in apparent conductivity, (b) geologic structures such as faults and karst can have detectable apparent conductivity signatures, and (c) conductivity measurements can be combined with geologic maps and outcrop studies to identify hidden contacts, covered strata, and unmapped structural features. Limited comparisons of measurements from ground and airborne instruments confirm that the instruments produce similar apparent conductivities at the same primary frequency and coil orientation. Ground instruments can be used to capture small-scale lateral conductivity change, complementing smoothed but spatially dense airborne measurements over large areas that are inaccessible or impractical to survey using ground-based instruments.

Page intentionally blank

INTRODUCTION

In 2002, the U.S. Geological Survey (USGS) conducted an airborne geophysical survey of the Seco Creek area in Medina and Uvalde Counties, Texas to better understand geological and hydrological issues relating to this important recharge area for the Edwards aquifer. We began working with the USGS in 2003 to conduct ground-based electromagnetic induction (EM) measurements in support of the airborne geophysical effort and to examine the influence of rock type and geological structure on the geophysical measurements.

Our field activities concentrated on Seco Creek and adjacent areas (fig. 1) because the area was accessible, we could make more detailed geophysical measurements and geological observations than are possible using airborne instruments or aerial photographs, and the creek is a critical recharge area for the Edwards aquifer.

Most ground-based EM measurements were made on Cretaceous strata or relatively thin alluvial deposits that form the creek bed. Quadrangle-scale geologic maps (Collins, 1997, 1998b, 1999a, b) show the bedrock geology to be dominated by the faulted limestones and dolomitic limestones and less common marls, shales, and mudstones of the lower Cretaceous Glen Rose and Devils River Formations and upper Cretaceous Del Rio and Buda Formations (fig. 2). In addition to these units, we also acquired EM data where Quaternary alluvium, alluvial terrace, and Leona Formation are mapped at the surface.

METHODS

We acquired measurements of apparent electrical conductivity in the Seco Creek area between May 19 and 23, 2003 using a Geonics EM34-3 ground conductivity meter. This instrument measures apparent electrical conductivity using the electromagnetic induction method (Parasnis, 1986; Frischknecht and others, 1991; and West and Macnae, 1991). The instrument, consisting of transmitter and receiver coils operating at primary frequencies of 400, 1600, and 6400 Hz, measures apparent conductivity by comparing the strength of a primary magnetic field

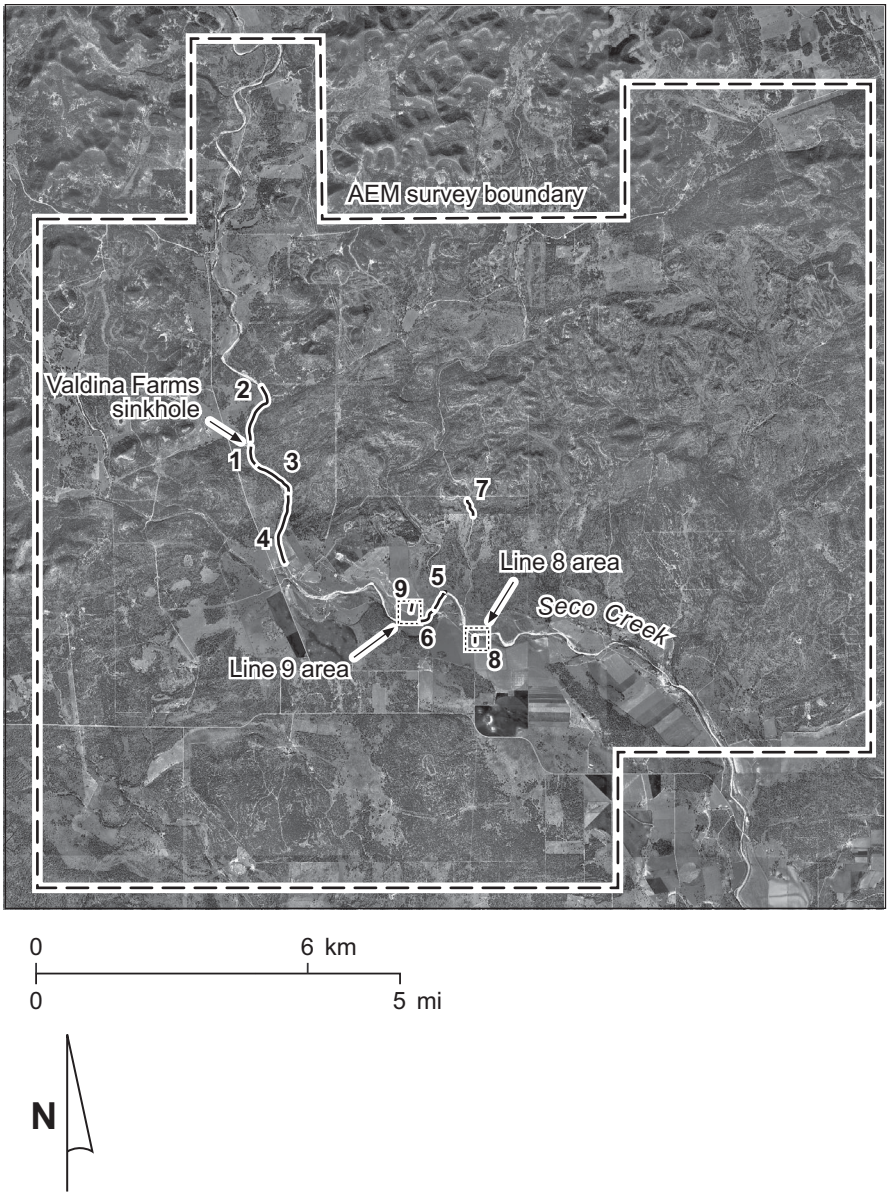

Figure 1. Aerial photomosaic of the Seco Creek area, Medina and Uvalde Counties, Texas showing the outline of the airborne survey and the locations of ground-based geophysical measurements. Aerial photographs modified from the Texas Natural Resource Information System.

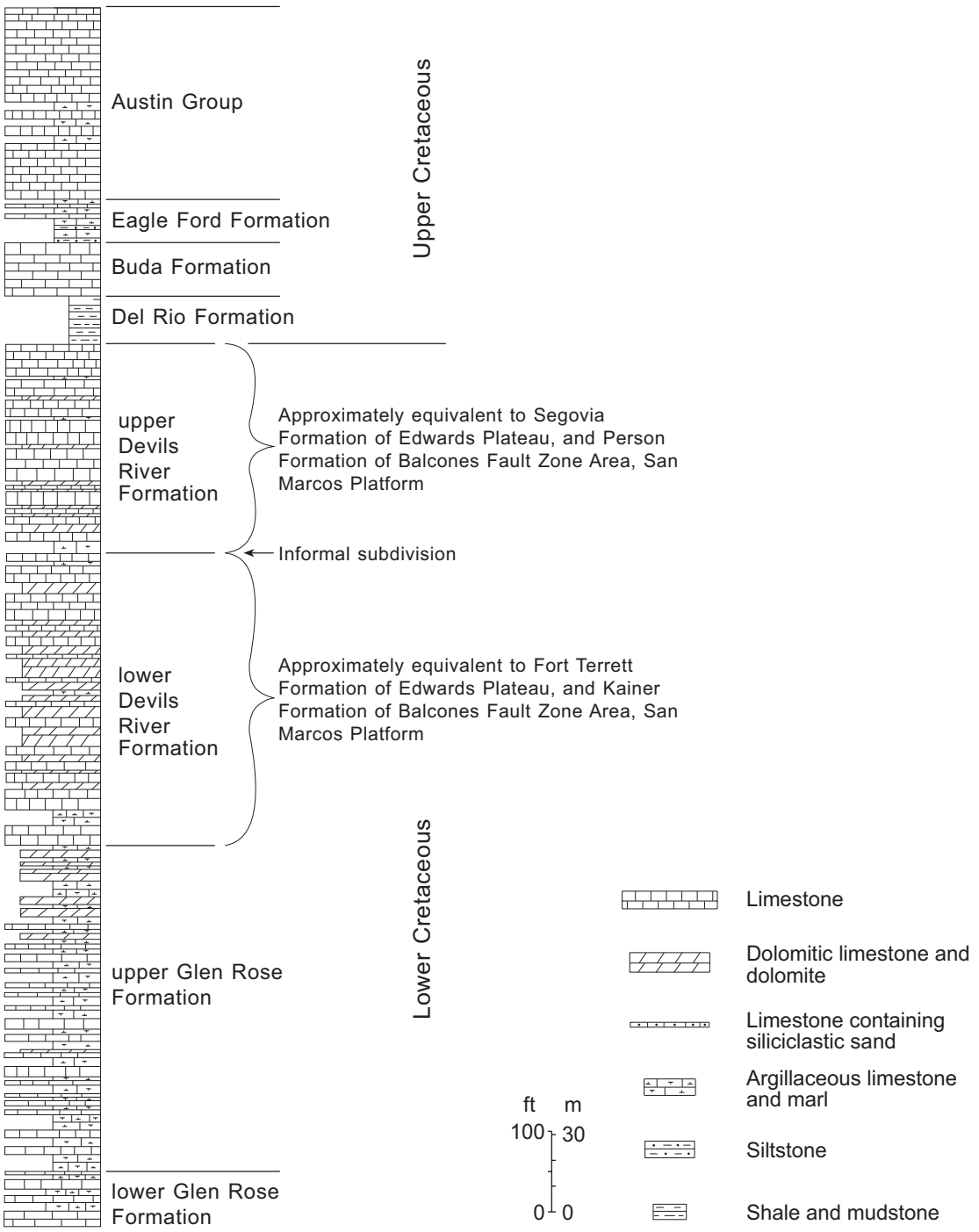

Figure 2. Generalized Cretaceous stratigraphy of the Seco Creek area. Modified from Collins (1998a).

generated by a sinusoidally varying current flowing in the transmitter coil to the magnetic field strength generated by secondary currents induced to flow in the ground by the changing primary field (McNeill, 1980). Exploration depth ranges from as shallow as the upper 6 m in the horizontal dipole coil orientation at 10 m coil separation to as deep as the upper 50 m in the vertical dipole coil orientation at 40 m coil separation (fig. 3).

We made stratigraphic and structural geologic observations and collected apparent conductivity measurements in the horizontal and vertical dipole coil orientations at 379 locations along 9 line segments on and near Seco Creek (fig. 1 and appendix). Most of these (lines 1 through 7) were reconnaissance measurements taken at a single coil separation (20 m) and station spacing (20 m). Data along lines 8 and 9 were acquired at 10-m station spacing and 10-, 20- and 40-m coil separations to enable construction of conductivity models. We used the program EMIX 34 Plus, published by Interpex, to analyze multiple-coil-separation data and produce best-fit conductivity models at four locations along these lines.

We determined station locations using a GPS receiver. Measurement locations are presented as the calculated centerpoint of the transmitter and receiver locations (appendix) and have been converted from original latitude and longitude values to the Universal Transverse Mercator projection, zone 14 north, using the 1927 North American Datum.

RESULTS

Lines 1, 2, 3, and 4: Seco Creek Near Valdina Farms Sinkhole

Lines 1, 2, 3, and 4 combine to form a nearly continuous apparent conductivity profile along Seco Creek from about 1.2 km upstream to 3.4 km downstream from the diversion dam at the Valdina Farms sinkhole (figs. 1 and 4a). Major geologic units traversed along this profile include the upper Glen Rose, lower Devils River, and Buda Formations (figs. 2 and 4b) as well as stream deposits of varying thickness and lateral extent (Collins, 1999a and b).

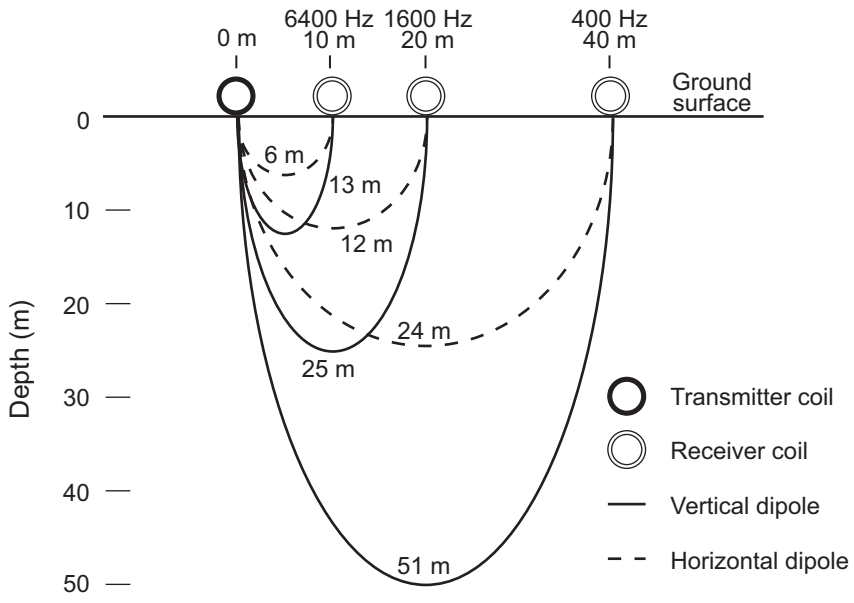

Figure 3. Exploration depth of various coil separations and orientations of the Geonics EM34-3 ground conductivity meter.

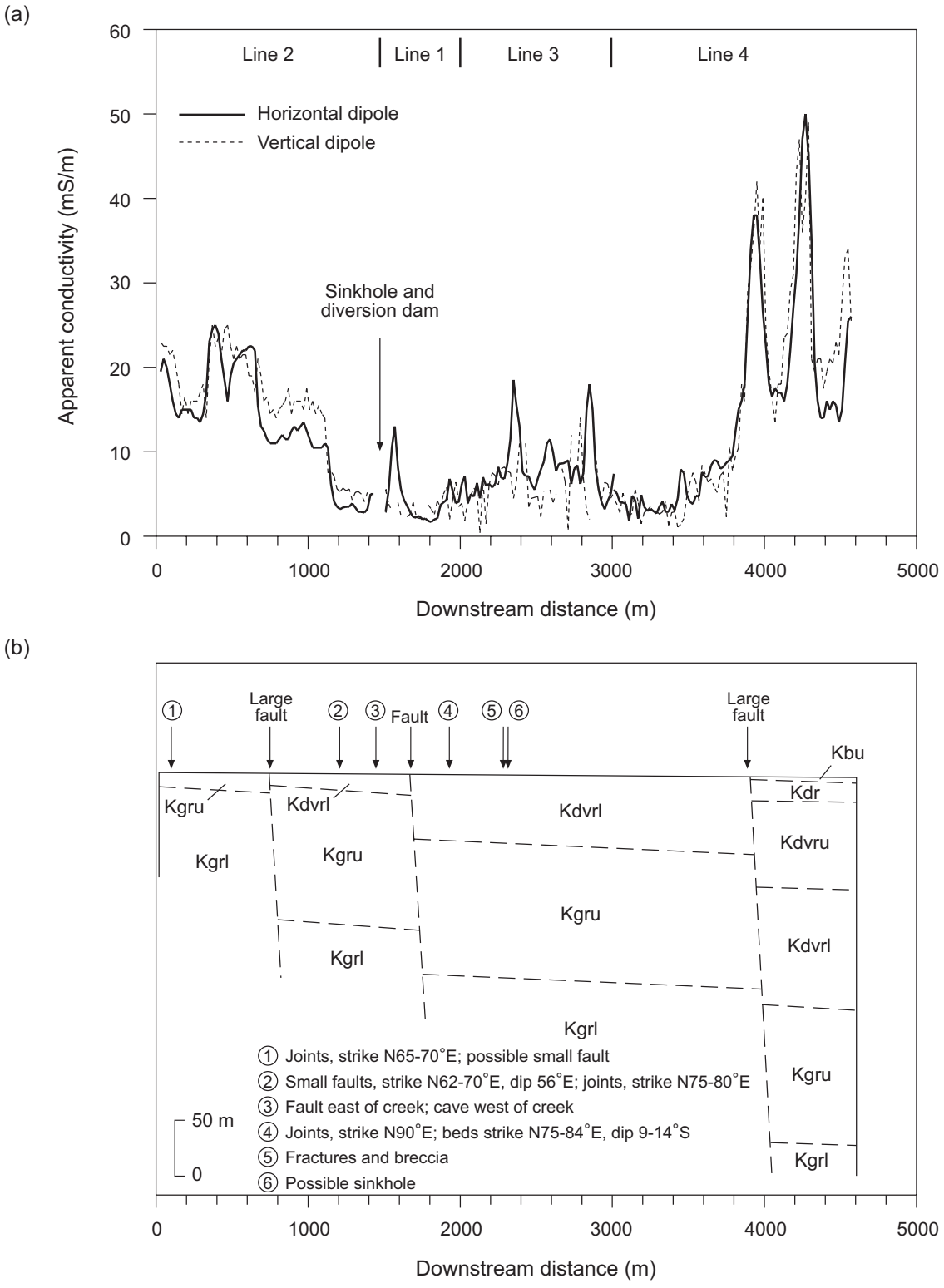

Figure 4. Relationship between apparent conductivity and geologic units along Seco Creek lines 1, 2, 3 and 4 upstream and downstream from the Valdina Farms sinkhole and diversion dam (fig. 1); (a) apparent conductivity measured using a ground-based instrument at 20-m coil separation; and (b) approximate geologic cross section and observed geologic features.

Apparent conductivities measured in the horizontal and vertical dipole orientations at 20-m coil spacing were generally low, ranging from a few to about 50 mS/m (fig. 4a). The lowest values (10 mS/m or less) were measured between downstream distances of 1.2 and 3.8 km, generally coinciding with the mapped extent of the lower Devils River Formation. This electrically resistive formation is largely composed of limestone, dolomitic limestone, and dolomite.

Higher apparent conductivities of 15 to 25 mS/m were measured along a 700-m-long segment at the upstream end of the profile (fig. 4a). Here the upper Glen Rose is the mapped bedrock unit (fig. 4b). This unit, consisting of interbedded limestone, dolomitic limestone, and argillaceous limestone and marl (fig. 2), should be more electrically conductive than strata dominated by limestone or dolomite owing to its locally higher clay and moisture content.

The highest and most variable apparent conductivities were measured at the downstream end of the profile (3.8 to 4.6 km, fig. 4a), where apparent conductivities of 15 to 20 mS/m are punctuated by higher values of 40 to 50 mS/m along short segments of the creek. The limestone-dominated Buda Formation is mapped along this stretch, suggesting that conductivity values should be low. Higher apparent conductivities may be the result of an instrument exploration depth of 12 to 25 m (fig. 3) that extends through thin Buda strata overlying the more conductive shale- and mudstone-dominated Del Rio Formation. Local conductivity highs may exist where alluvium is thick or where Del Rio strata have been brought to the surface along small faults.

In addition to the apparent correlation between rock type and measured conductivity, other geologic features are represented in the conductivity data. Large mapped faults, such as those juxtaposing upper Glen Rose and lower Devils River strata at a downstream distance of 800 m and lower Devils River and Buda or Del Rio strata at about 4 km (fig. 4), are accompanied by abrupt changes in measured conductivity. Unmapped faults may be identified by similar abrupt conductivity changes such as those observed at locations 1 and 2 (fig. 4b) where small faults and joints are common. Local conductivity highs in generally nonconductive strata at locations 5 and 6 (fig. 4b) coincide with fractures, brecciation, and increased clay content associated with a paleokarst feature.

Lines 5 and 6: Seco Creek Near Parkers Creek Confluence

We acquired lines 5 and 6 along a 0.9-km-long segment of Seco Creek upstream from its confluence with Parkers Creek. Line 5 (the downstream segment) is separated from line 6 (the upstream segment) by a failed concreted bridge. Horizontal and vertical dipole conductivity data were acquired at 20-m coil separation and station spacing. Quaternary alluvial deposits are mapped along this profile (Collins, 1998b).

Apparent conductivities generally decrease downstream along this profile (fig. 5). Upstream from the bridge, relatively high conductivities of 25 to 60 mS/m were measured, consistent with the inferred presence of conductive Del Rio Formation bedrock at shallow depths beneath alluvium. Downstream from the bridge, measured conductivities decrease from about 20 mS/m at 500 m to less than 10 mS/m beyond 700 m (fig. 5). These low conductivities are consistent with the presence of resistive carbonates of the upper Devils River Formation at the surface or beneath a thin alluvial veneer.

Line 7: Across Inferred Fault

We acquired line 7 along an unnamed drainage east of Parkers Creek (fig. 1) using the 20-m coil separation and a 20-m station spacing. This line crosses an inferred fault at about 120 m from the south end of the line. The inferred fault separates upper Devils River strata south of the fault from lower Devils River strata north of the fault (Collins, 1997).

Measured apparent conductivities are low along the entire 400-m length of the profile (fig. 6). Apparent conductivities are below 5 mS/m at the south end of the line, but gradually increase northward beginning about 50 m north of the inferred fault location. Slightly higher apparent conductivities were measured north of the inferred fault, where the lower Devils River Formation is mapped.

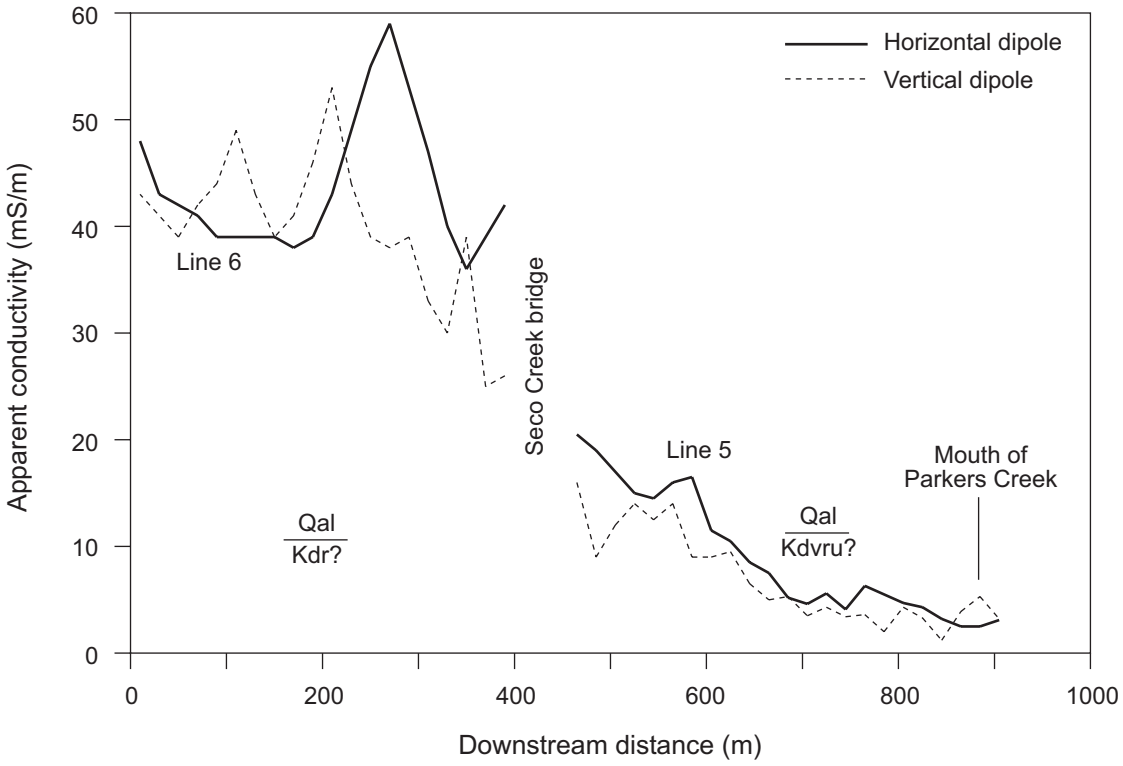

Figure 5. Apparent conductivity measured along Seco Creek lines 5 and 6 (fig. 1) using a ground-based instrument at 20-m coil separation.

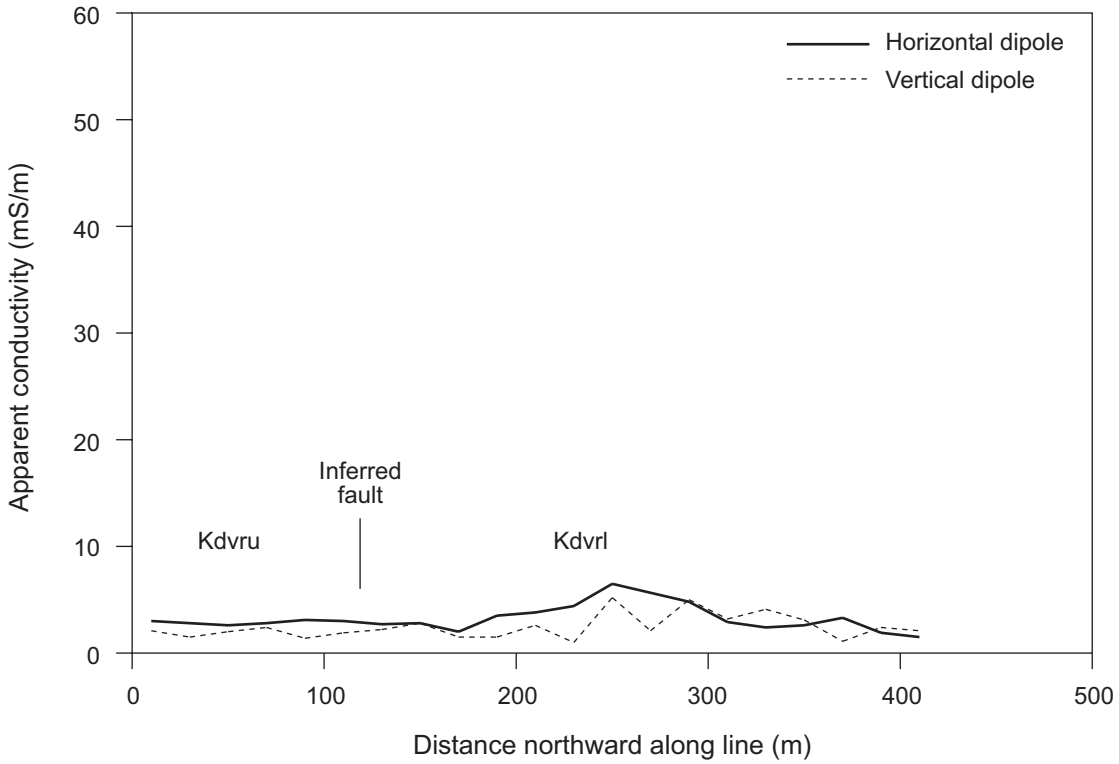

Figure 6. Apparent conductivity measured along line 7 (fig. 1) using a ground-based instrument at 20-m coil separation. Stratigraphic units and inferred fault position from Collins (1997).

Line 8: Terrace South of Seco Creek

Line 8 is a 120-m long profile located on a terrace south of Seco Creek (figs. 1 and 7). We acquired apparent conductivity data along this line at 10-, 20-, and 40-m coil separations and a 10-m station spacing for each coil separation (fig. 8 and appendix). The terrace is mapped as the Leona Formation (Collins, 1998b), a Quaternary alluvial unit with low surface relief situated several meters above Seco Creek and its modern alluvial deposits.

Along the northern 60 m of the line, apparent conductivities are relatively constant at each coil separation (fig. 8). At the 10-m separation, measured conductivities are between 20 and 30 mS/m, increasing to more than 30 mS/m at the deeper exploring 20- and 40-m separations. Farther south, all apparent conductivities measured in the horizontal dipole mode show significant increases, reaching 70 mS/m at the north end of the line for the 10- and 20-m coil separations. The shallowest-exploring vertical dipole configuration also depicts a southward increase in apparent conductivity, but the 20- and 40-m vertical dipole data do not.

Relatively high apparent conductivities along line 8 are consistent with typical values for alluvial deposits with varying water saturation. Southward decreases that are most apparent at shallow exploration depths may be caused by increasing unsaturated zone thickness as the distance to the edge of the terrace decreases, or to a significant southward increase in clay content in shallow strata.

Comparison with Airborne Measurements

We compared apparent conductivities measured using a ground instrument along line 8 with the nearest available measurements made using an airborne sensor on a parallel flight line (figs. 7 and 9). Flight line 10500 crosses a similar geologic environment, but is about 150 m east of line 8. Given the large observed lateral variation along line 8, the comparison may not be valid.

We compared data from the airborne 6200 Hz coils (vertical dipole orientation) with the 10-m coil separation (6400 Hz) horizontal and vertical dipole data (fig. 9a), data from the air-

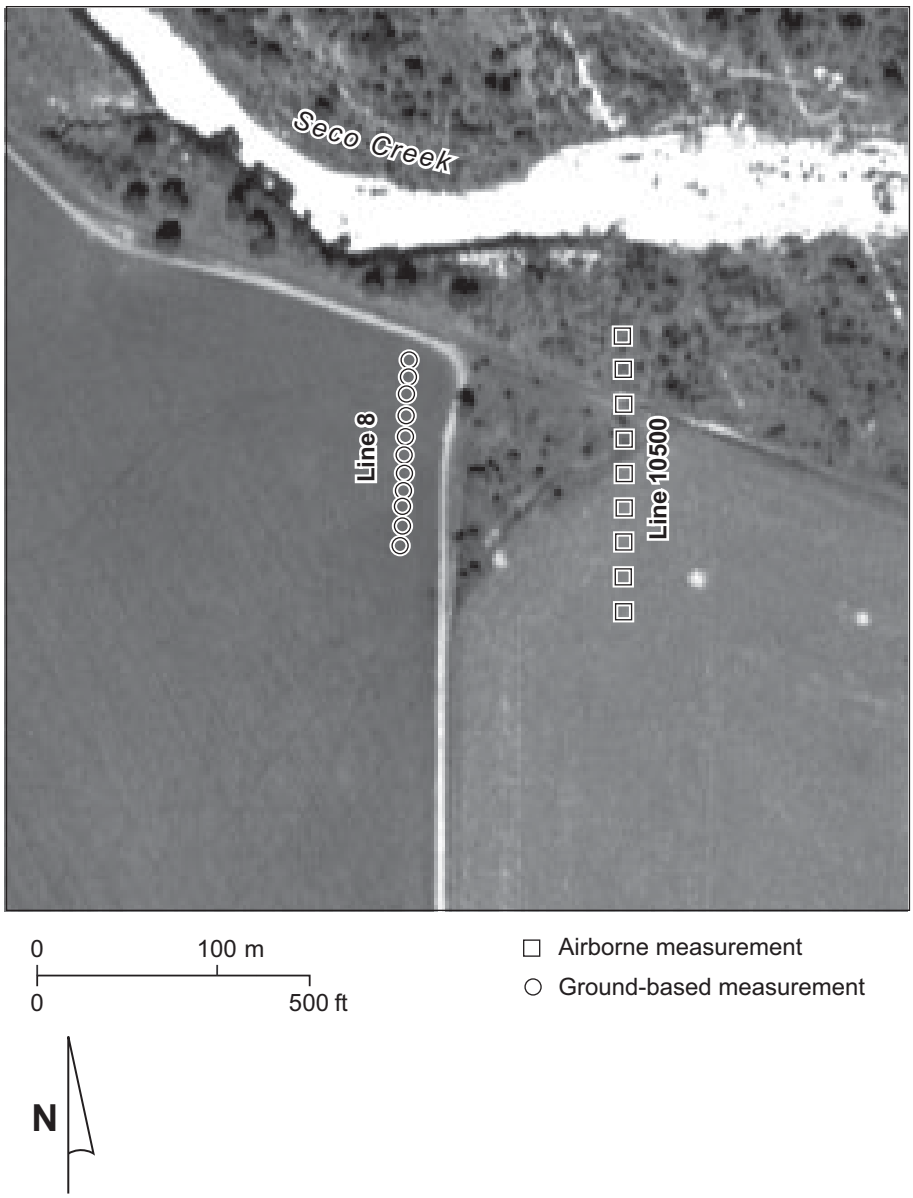

Figure 7. Aerial photograph showing line 8 from the ground-based EM survey and a correlative segment of line 10500 from the airborne geophysical survey.

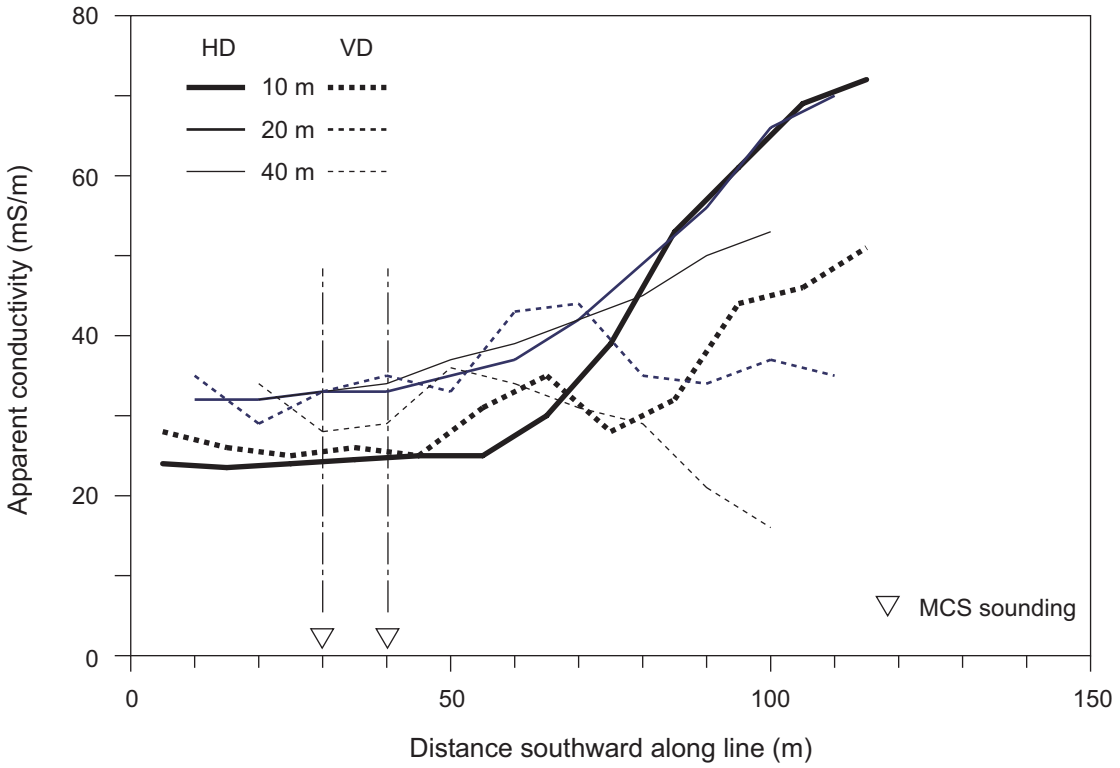

Figure 8. Apparent conductivity measured along line 8 (fig. 1) using a ground-based instrument at 10-, 20-, and 40-m coil separations. Also shown are the locations of two vertical conductivity profiles constructed from multiple-coil-separation measurements.

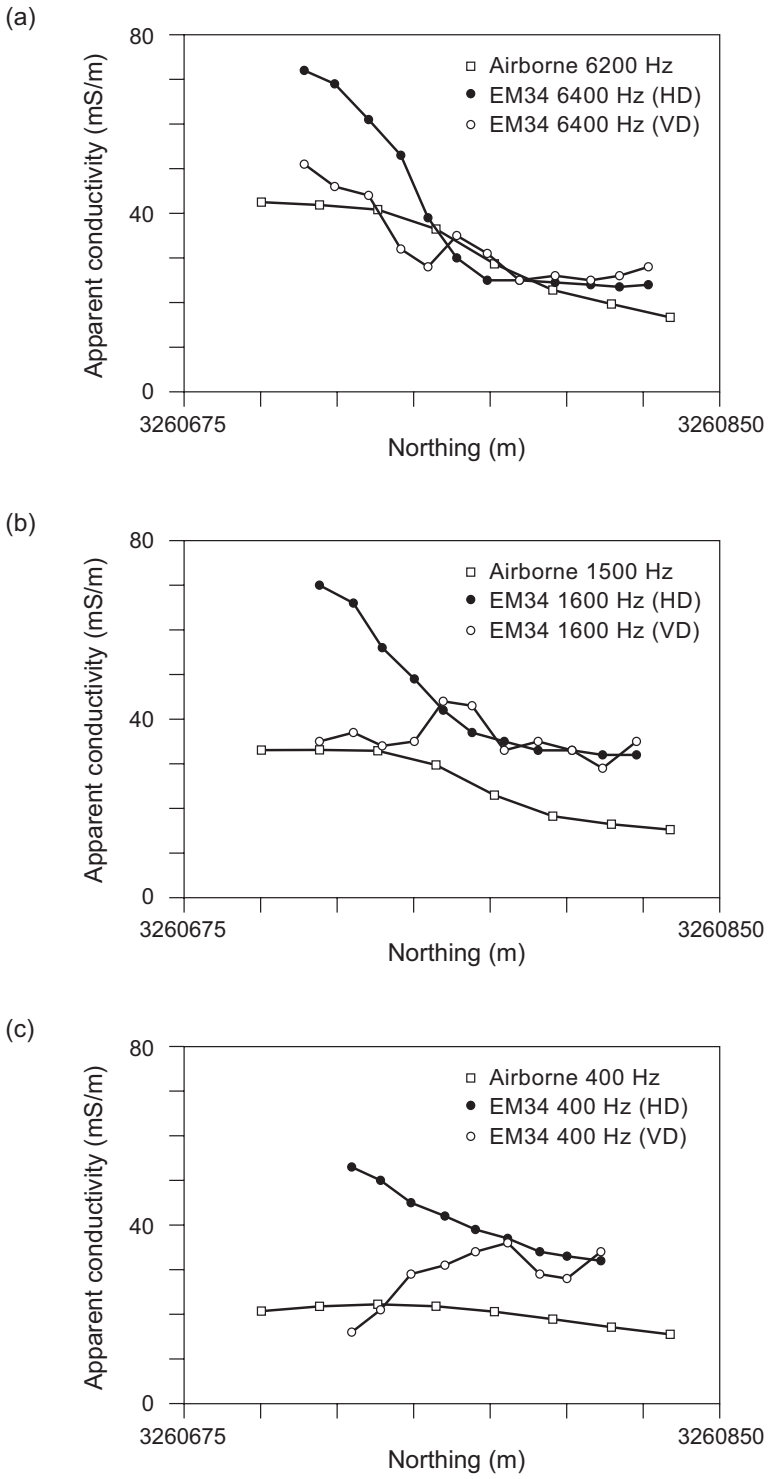

Figure 9. Comparison of apparent conductivities along lines 8 (ground) and 10500 (airborne). (a) Apparent conductivity measured using a ground instrument at 10-m coil separation (6400 Hz) and an airborne instrument at 6200 Hz; (b) apparent conductivity measured using a ground instrument at 20-m coil separation (1600 Hz) and an airborne instrument at 1600 Hz; and (c) apparent conductivity measured using a ground instrument at 40-m coil separation (400 Hz) and an airborne instrument at 400 Hz.

borne 1600 Hz coils with the 20-m coil separation (1600 Hz) ground data (fig. 9b), and data from the airborne 400 Hz coils with the 40-m coil separation (400 Hz) ground data (fig. 9c). At each of the three primary frequencies, airborne instruments depict more smoothly varying apparent conductivities, confirming that ground instruments can achieve higher lateral resolution than similar airborne instruments.

At 6200 Hz primary frequency, airborne measurements most closely match the 6400 Hz vertical dipole apparent conductivities measured using the ground instrument (fig. 9a). At 1600 Hz, airborne measurements are nearly identical to ground measurements at the same frequency and vertical dipole orientation at the south end of the line, but diverge toward the north end where there is a loss of surface elevation on line 10500. Airborne and ground measurements are most different at 400 Hz (fig. 9c), where the trend (but not the magnitude) of the airborne measurements is similar to that of the horizontal dipole ground measurements. The magnitude (but not the trend) of the airborne measurements is most similar to that of the vertical dipole ground measurements.

Vertical Profiles

We constructed best-fit vertical conductivity profiles at two locations along line 8 where lateral apparent conductivity change was minimal. These adjacent locations are 30 and 40 m from the north end of the line (fig. 8), where apparent conductivities are relatively low.

We used horizontal and vertical dipole data at the three coil separations to create the models and calculate the fitting errors. At 30 m, a three-layer model produced a fitting error of 2.2 percent between actual and synthetic apparent conductivities (fig. 10). This model consisted of a relatively resistive (26 mS/m) surface layer 11 m thick, an underlying conductive (104 mS/m) layer about 13 m thick, and a basal resistive (4 mS/m) layer of undetermined thickness. The adjacent model at 40 m is similar (fig. 11), having a slightly thicker surface resistive layer, a slightly thinner but more conductive intermediate layer, and a lower fitting error of 1.5 percent.

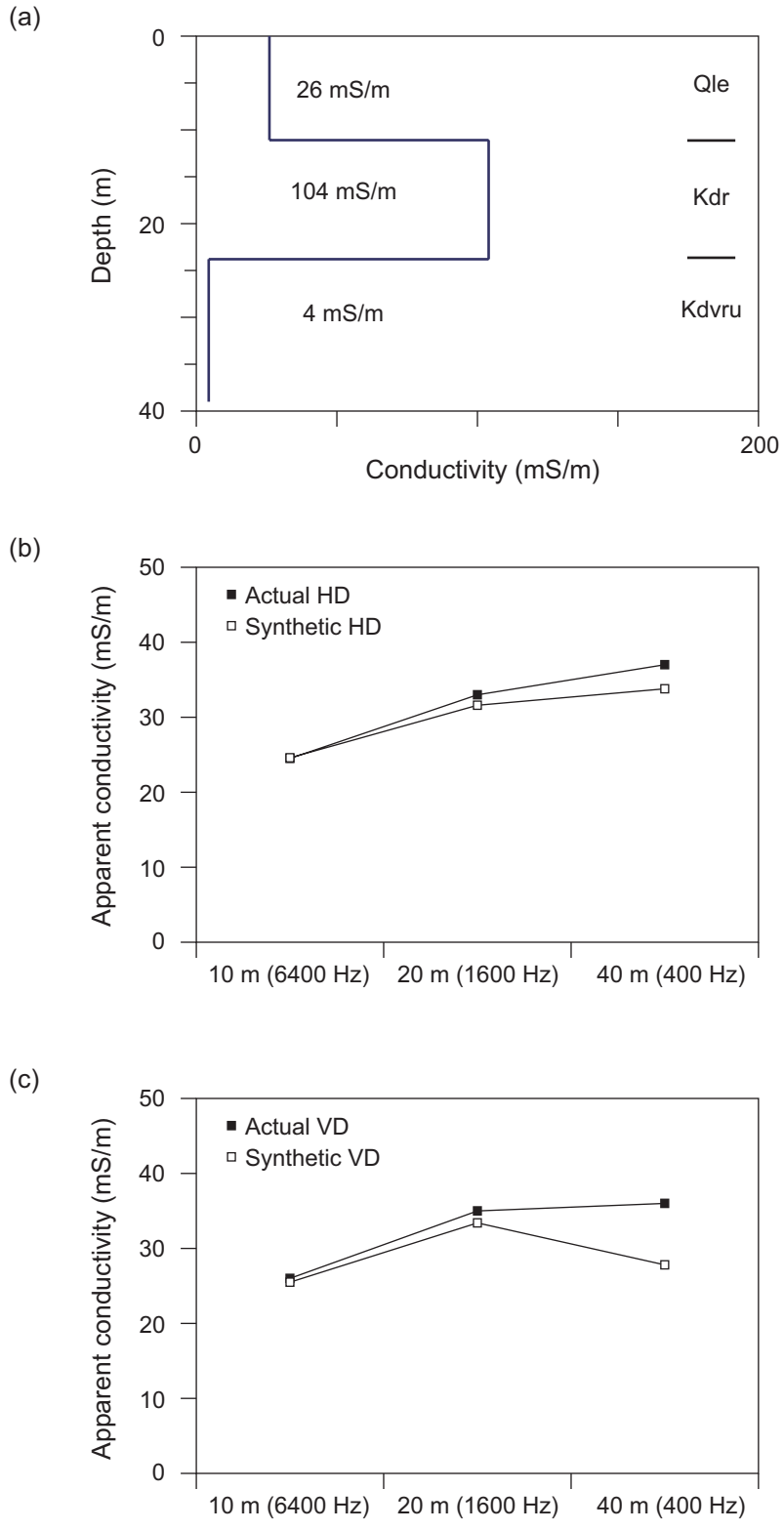

Figure 10. Calculated vertical conductivity profile at 30 m on line 8. (a) Vertical conductivity profile showing interpreted geologic units; (b) actual and synthetic horizontal dipole apparent conductivities; and (c) actual and synthetic vertical dipole apparent conductivities.

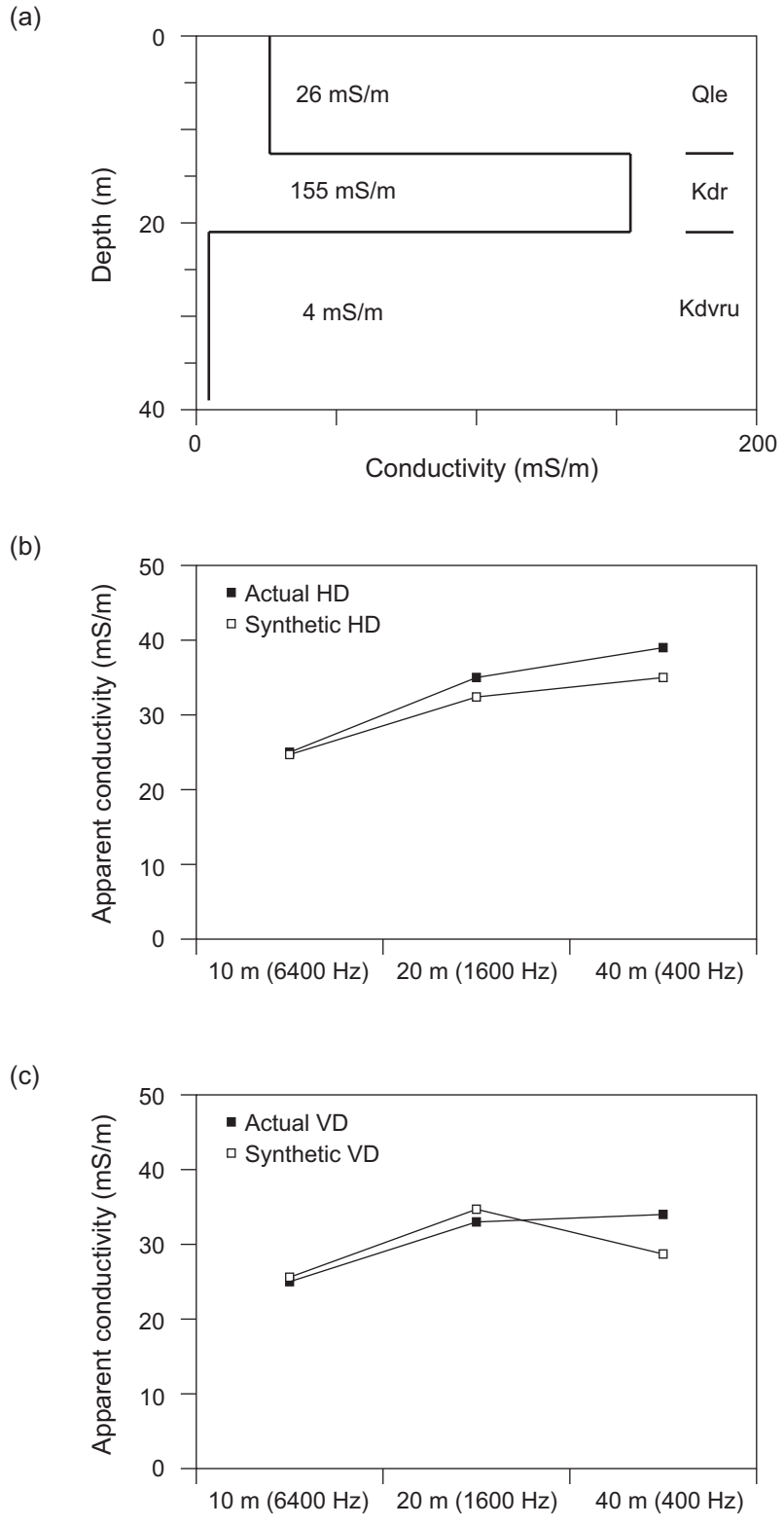

Figure 11. Calculated vertical conductivity profile at 40 m on line 8. (a) Vertical conductivity profile showing interpreted geologic units; (b) actual and synthetic horizontal dipole apparent conductivities; and (c) actual and synthetic vertical dipole apparent conductivities.

One possible geologic interpretation of these models is that the surface layer represents Leona Formation alluvium, the intermediate layer represents relatively conductive Del Rio strata, and the basal unit represents highly resistive upper Devils River carbonate strata.

Line 9: Terraces North of Seco Creek

Line 9 extends northerly about 200 m across parts of two terraces on the north side of Seco Creek upstream from the Parkers Creek confluence (figs. 1 and 12). We acquired horizontal and vertical dipole apparent conductivity measurements at 10-, 20-, and 40-m coil separations and a 10-m station spacing. The southern half of the line was acquired across an area mapped as a Quaternary alluvial terrace (fig. 13). The northern half of the line climbs about 3 m in elevation, ending on a higher Quaternary alluvial terrace mapped as the Leona Formation (Collins, 1998b). Buda Formation limestone is exposed in Seco Creek about 200 m south of line 9.

Measured apparent conductivities showed relatively little change along this line (fig. 13). Most measurements were between 15 and 20 mS/m across the lower terrace (0 to 110 m, fig. 13). On the higher terrace near the north end of the line, horizontal dipole apparent conductivities showed a northward increase that reflects increasing conductivities in the shallow subsurface, but apparent conductivities remain below 30 mS/m in all configurations.

We constructed best-fit vertical conductivity profiles at two locations on line 9 where lateral apparent conductivity changes were minor. One profile, located at 50 m on the lower terrace (figs. 13 and 14), included three layers that produced a 3 percent fitting error between actual and synthetic apparent conductivities for all coil spacings and orientations. The model (fig. 14a) includes a surface resistive (8 mS/m) layer that is about 5 m thick, an underlying conductive (46 mS/m) layer that is 15 m thick, and a basal, highly resistive (0.2 mS/m) layer. Considering the conductivities and thicknesses of the layers and the geologic setting, a reasonable geologic interpretation (fig. 14a) is that the surface layer represents relatively dry Quaternary alluvial deposits and perhaps a thin remnant of Buda Formation carbonates, the intermediate layer repre-

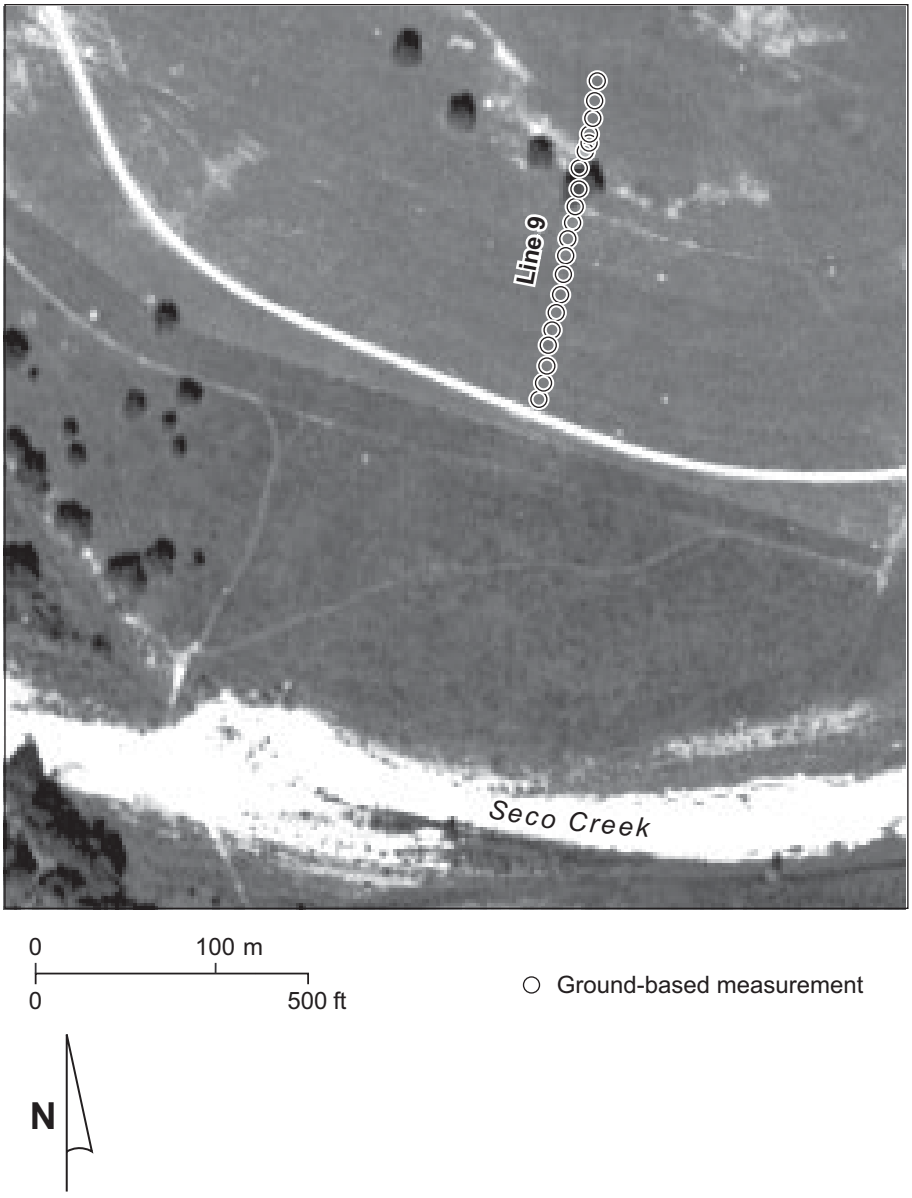

Figure 12. Aerial photograph showing line 9 from the ground-based EM survey.

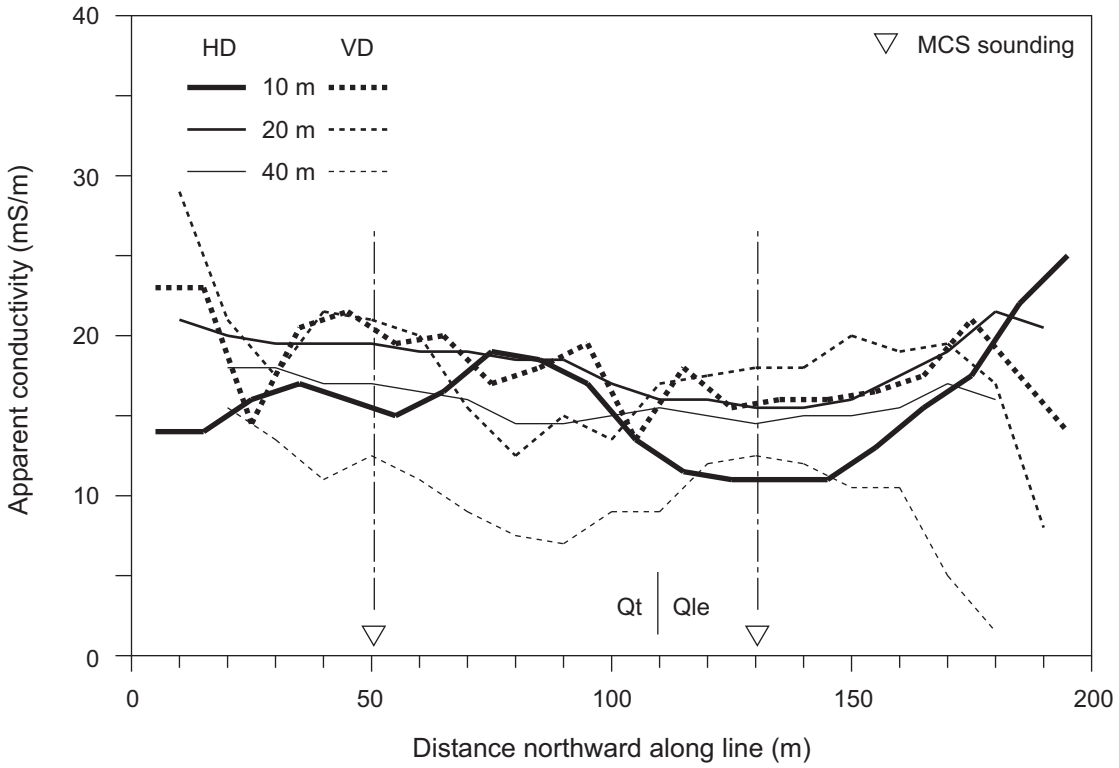

Figure 13. Apparent conductivity measured along line 9 (fig. 1) using a ground-based instrument at 10-, 20-, and 40-m coil separations. Also shown are the locations of two vertical conductivity profiles constructed from multiple-coil-separation measurements. Approximate Qt and Qle contact from Collins (1998b).

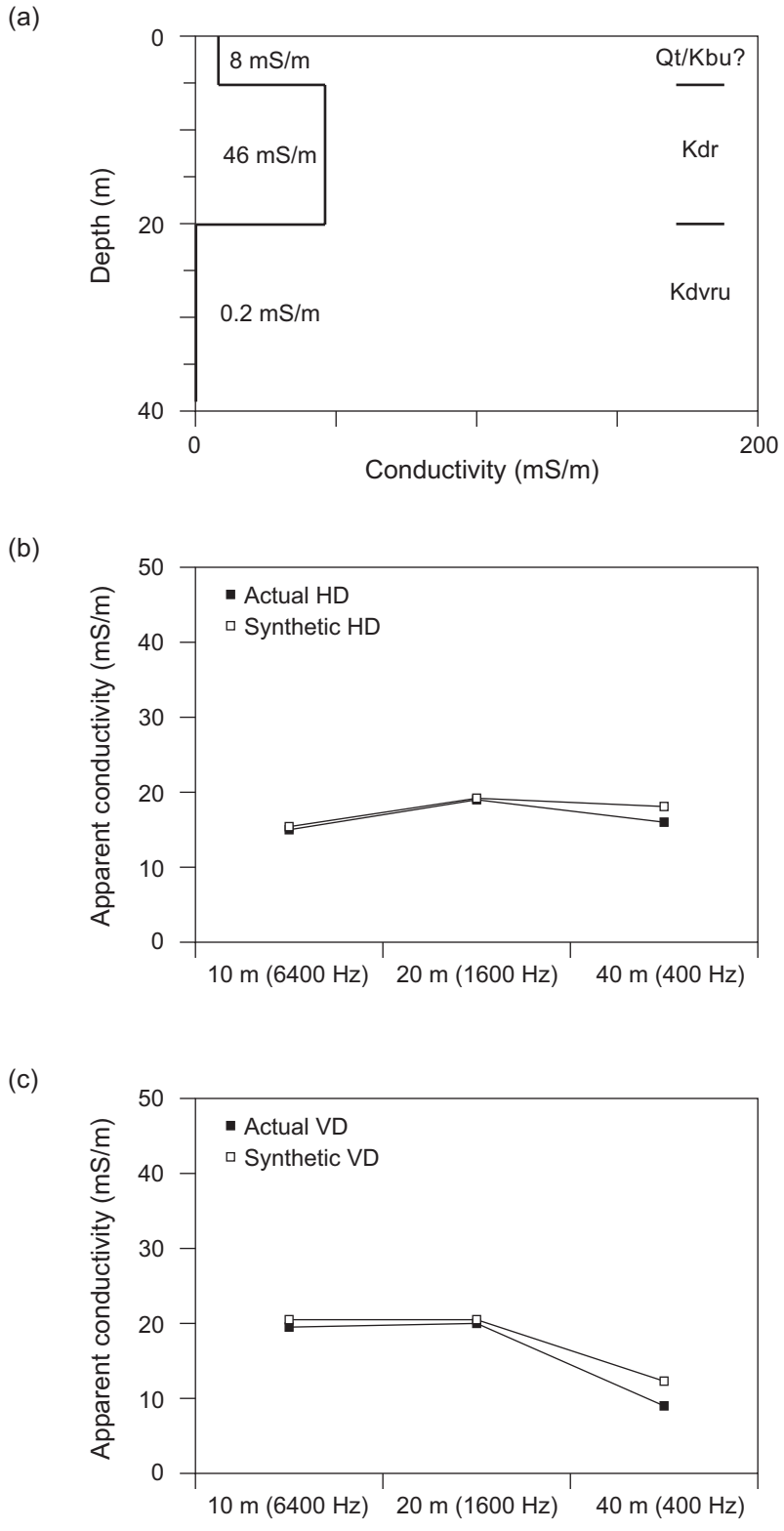

Figure 14. Calculated vertical conductivity profile at 50 m on line 9. (a) Vertical conductivity profile showing interpreted geologic units; (b) actual and synthetic horizontal dipole apparent conductivities; and (c) actual and synthetic vertical dipole apparent conductivities.

sents the more conductive Del Rio Formation, and the basal resistive layer represents poorly conductive carbonates of the upper Devils River Formation.

The vertical profile at 130 m (figs. 13 and 15) is located on the higher terrace mapped as the Leona Formation. The three-layer, best-fit conductivity model is similar to the one at 30 m. Differences include a slightly less conductive and thicker surface layer (5 mS/m, 6 m) and intermediate layer (38 mS/m, 17 m) and a slightly more conductive basal unit (2 mS/m). The fitting error remains 3 percent. A geologic interpretation similar to that at 30 m is plausible, except that the surface layer represents Leona rather than lower terrace strata.

CONCLUSIONS

Geologic observations and ground-based geophysical measurements combined with existing geologic mapping and airborne geophysical measurements provide an iterative means of understanding the geological and hydrological setting of the Seco Creek area and add geological and hydrological meaning to geophysical data. Ground-based measurements acquired along and near Seco Creek confirm that rock type changes are reflected in measured conductivity values, structural features such as faults can be identified, and karst structures can be associated with conductivity anomalies. Multi-frequency ground-conductivity data can be used to construct simple vertical conductivity models that can be interpreted geologically where sufficient conductivity contrasts exist among strata within the exploration depth of the instrument. Ground-based and airborne instruments appear to produce similar apparent conductivity measurements for similar coil orientations and frequencies. Ground-based instruments can achieve higher lateral resolution than can airborne instruments, but airborne instruments provide areal coverage that is unachievable on the ground.

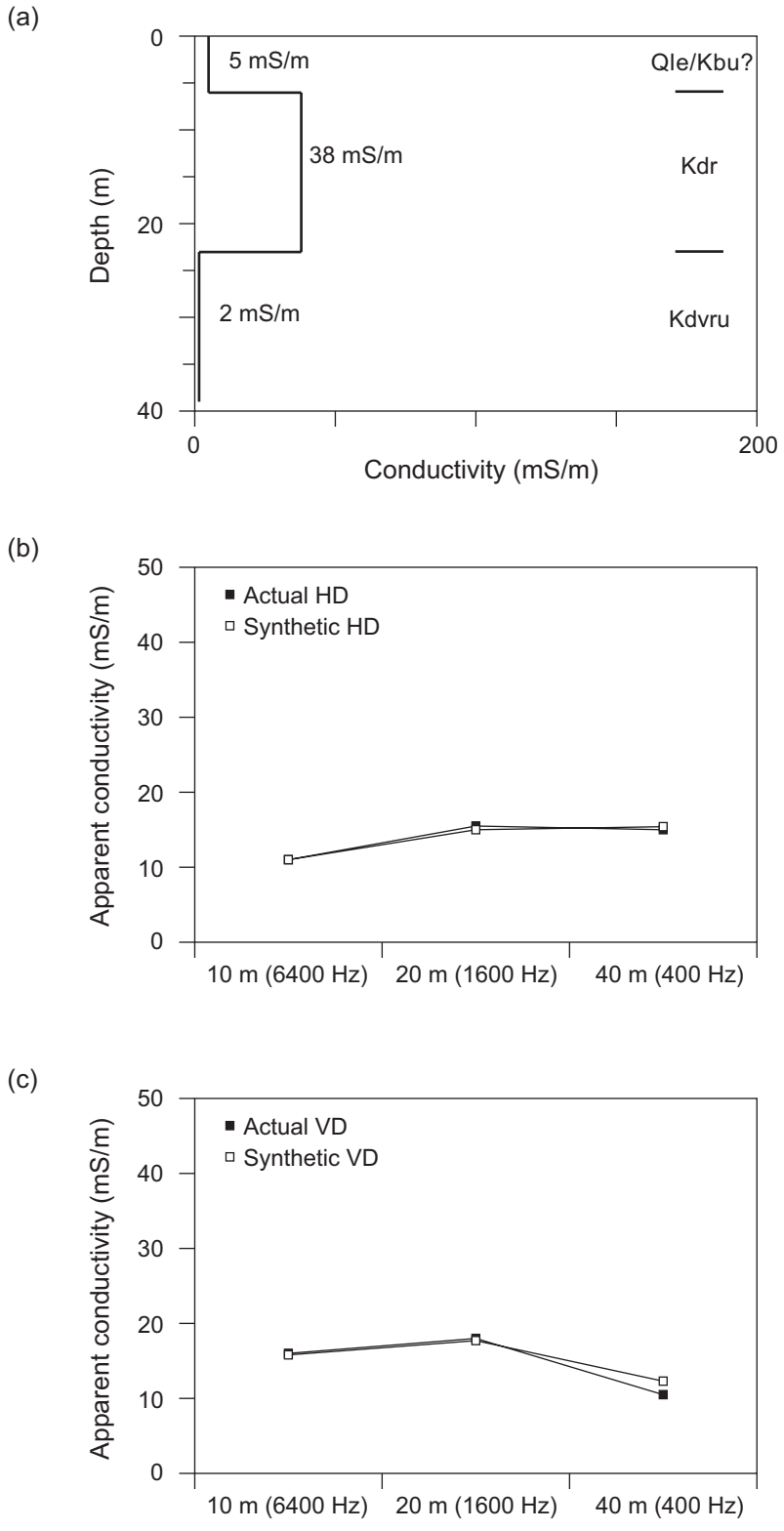

Figure 15. Calculated vertical conductivity profile at 130 m on line 9. (a) Vertical conductivity profile showing interpreted geologic units; (b) actual and synthetic horizontal dipole apparent conductivities; and (c) actual and synthetic vertical dipole apparent conductivities.

ACKNOWLEDGMENTS

This study was partly supported by the U.S. Geological Survey (USGS) under order no. 02CRSA0768. Bruce Smith (USGS) served as project manager, arranged land access, and provided airborne geophysical data. We thank Virgil Boll for granting access to Valdina Farms for ground-based geophysical measurements and geological observations.

REFERENCES

Collins, E. W., 1997, Geologic map of the Texas Mountain quadrangle, Texas: The University of Texas at Austin, Bureau of Economic Geology, open-file map prepared for the U.S. Geological Survey under cooperative agreement no. 1434-HO-96-AG-01518, 1 sheet, scale 1:24,000.

Collins, E. W., 1998a, Environmental geology of urban growth areas within the Edwards aquifer and Balcones Fault Zone, South-Central Texas (poster and ext. abs.): Gulf Coast Association of Geological Societies Transactions, v. 48, p. 537-538.

Collins, E. W., 1998b, Geologic map of the Sabinal NE quadrangle, Texas: The University of Texas at Austin, Bureau of Economic Geology, open-file map prepared for the U.S. Geological Survey under cooperative agreement no. 1434-HQ-97-AG-01765, 1 sheet, scale 1:24,000.

Collins, E. W., 1999a, Geologic map of the Comanche Waterhole quadrangle, Texas: The University of Texas at Austin, Bureau of Economic Geology, open-file map prepared for the U.S. Geological Survey under cooperative agreement no. 98HQAG2040, 1 sheet, scale 1:24,000.

Collins, E. W., 1999b, Geologic map of the Flat Rock Crossing quadrangle, Texas: The University of Texas at Austin, Bureau of Economic Geology, open-file map prepared for the U.S. Geological Survey under cooperative agreement no. 98HQAG2040, 1 sheet, scale 1:24,000.

Frischknecht, F. C., Labson, V. F., Spies, B. R., and Anderson, W. L., 1991, Profiling using small sources, *in* Nabighian, M. N., ed., Electromagnetic methods in applied geophysics—applications, part A and part B: Tulsa, Society of Exploration Geophysicists, p. 105-270.

McNeill, J. D., 1980, Electromagnetic terrain conductivity measurements at low induction numbers: Geonics Ltd., Mississauga, Ontario, Canada, Technical Note TN-6, 15 p.

Parasnis, D. S., 1986, Principles of Applied Geophysics: Chapman and Hall, 402 p.

West, G. F., and Macnae, J. C., 1991, Physics of the electromagnetic induction exploration method, *in* Nabighian, M. N., ed., Electromagnetic methods in applied geophysics—applications, part A and part B: Tulsa, Society of Exploration Geophysicists, p. 5-45.

Page intentionally blank

APPENDIX: GROUND-BASED EM DATA

Horizontal (HD) and vertical (VD) dipole apparent conductivities measured in the Seco Creek area using a Geonics EM34-3 ground conductivity meter. Measurement locations are the calculated midpoint between transmitter and receiver coil positions in decimal degrees (unprojected) and in meters using the Universal Transverse Mercator projection, zone 14 north, 1927 North American Datum. Locations and elevations calculated from GPS data. Line locations on fig. 1.

Line 1

Acquired May 19, 2003

20 m coil separation; 1600 Hz primary frequency

Latitude (° north)	Longitude (° west)	Easting (m)	Northing (m)	Elevation (m)	HD app. cond. (mS/m)	VD app. cond. (mS/m)
29.51598	99.39771	461456.9	3265219.9	383	2.9	5.5
29.51580	99.39775	461453.4	3265200.0	381	5.5	3.8
29.51562	99.39777	461450.9	3265179.5	381	10.5	3
29.51543	99.39782	461446.0	3265159.0	381	13	
29.51520	99.39783	461444.9	3265133.5	383	8.2	4
29.51516	99.39791	461437.6	3265129.1	386	5.6	2.5
29.51507	99.39791	461437.1	3265118.6	385	4.3	
29.51471	99.39776	461451.5	3265079.2	385	3.6	2.3
29.51453	99.39773	461454.4	3265058.7	383	2.9	2.6
29.51442	99.39773	461454.3	3265046.5	382	2.3	4
29.51425	99.39767	461460.6	3265028.2	381	2.2	2.4
29.51405	99.39762	461465.3	3265005.5	379	2.4	2.1
29.51385	99.39759	461467.7	3264983.3	376	2	2.2
29.51368	99.39752	461474.9	3264965.0	376	2.1	
29.51352	99.39745	461481.6	3264946.7	376	1.8	3.7
29.51334	99.39738	461488.3	3264926.7	375	1.7	3.2
29.51318	99.39729	461496.5	3264909.5	375	2	2.6
29.51304	99.39720	461505.2	3264894.0	375	2.1	4.2
29.51290	99.39709	461515.8	3264878.4	374	3.7	3.4
29.51277	99.39696	461528.8	3264863.4	374	4	5
29.51263	99.39680	461544.3	3264847.8	375	4.3	5.8
29.51250	99.39664	461559.7	3264833.9	375	6.8	2
29.51238	99.39648	461574.7	3264820.6	374	5.4	4.3
29.51224	99.39631	461591.1	3264804.5	372	3.9	6.4
29.51207	99.39613	461608.5	3264785.6	370	4.1	4.2

Line 2

Acquired May 20, 2003

20 m coil separation; 1600 Hz primary frequency

Latitude (° north)	Longitude (° west)	Easting (m)	Northing (m)	Elevation (m)	HD app. cond. (mS/m)	VD app. cond. (mS/m)
29.51739	99.39786	461443.3	3265376.2	361	5	4.5
29.51756	99.39787	461442.0	3265395.0	362	5	
29.51776	99.39791	461438.6	3265417.2	361	3.2	5.2
29.51787	99.39795	461434.3	3265429.4	361	2.8	4.1

29.51803	99.39799	461430.5	3265447.1	361	2.9	5
29.51828	99.39802	461427.7	3265474.8	361	2.9	5.3
29.51849	99.39798	461431.6	3265497.5	362	3.4	5.2
29.51866	99.39797	461433.2	3265516.9	361	3.9	4.3
29.51881	99.39805	461425.5	3265533.0	359	3.5	5.6
29.51898	99.39809	461421.2	3265552.4	358	3.5	5.4
29.51919	99.39811	461419.3	3265575.1	358	3.4	5.7
29.51933	99.39813	461417.4	3265591.2	358	3.2	5.3
29.51949	99.39814	461416.5	3265608.9	359	3.5	5.6
29.51970	99.39810	461420.5	3265632.2	359	4.1	7.1
29.51987	99.39806	461424.4	3265651.0	359	6.2	7.7
29.52006	99.39805	461425.5	3265671.5	360	10.5	7.5
29.52023	99.39803	461427.5	3265690.9	358	11	14
29.52039	99.39799	461431.4	3265708.1	356	10.5	14.5
29.52057	99.39794	461436.3	3265728.5	356	10.5	15.5
29.52075	99.39787	461443.6	3265747.9	356	10.5	14.5
29.52091	99.39778	461452.4	3265765.6	355	10.5	16
29.52107	99.39767	461463.1	3265783.3	356	11.5	15
29.52123	99.39759	461470.5	3265801.0	355	12.5	17.5
29.52140	99.39752	461477.8	3265819.8	354	13.5	15
29.52155	99.39741	461488.0	3265837.0	355	13	16
29.52170	99.39732	461497.3	3265853.0	354	12.5	16
29.52185	99.39723	461505.6	3265869.6	353	13	16
29.52205	99.39720	461509.1	3265891.7	354	12.5	14.5
29.52223	99.39713	461515.9	3265911.6	353	11.5	17.5
29.52236	99.39703	461525.2	3265926.0	353	11.5	16
29.52253	99.39695	461533.5	3265944.8	353	12	15.5
29.52269	99.39685	461543.2	3265963.1	353	11.5	15
29.52285	99.39675	461552.5	3265980.8	353	11	14
29.52301	99.39672	461555.9	3265998.5	353	11	15
29.52317	99.39663	461564.2	3266016.2	354	11	14.5
29.52333	99.39646	461581.3	3266033.9	353	11.5	16.5
29.52347	99.39633	461593.4	3266049.3	353	12.5	16
29.52368	99.39619	461607.6	3266072.0	354	13	19
29.52384	99.39602	461624.1	3266089.7	356	15.5	21
29.52393	99.39589	461636.2	3266099.6	357	22	17
29.52403	99.39577	461648.4	3266110.6	357	22.5	19
29.52411	99.39562	461663.0	3266120.0	356	22.5	19
29.52421	99.39545	461679.0	3266130.5	355	22	21.5
29.52432	99.39528	461695.5	3266143.2	354	22	21.5
29.52443	99.39511	461712.5	3266154.7	353	21.5	21
29.52448	99.39492	461730.9	3266160.2	354	21	22.5
29.52454	99.39473	461749.4	3266166.8	353	20.5	21
29.52460	99.39454	461767.8	3266173.9	352	19	22.5
29.52467	99.39434	461786.7	3266181.6	353	16	25
29.52474	99.39416	461804.2	3266188.8	355	18.5	24.5
29.52486	99.39404	461815.9	3266202.6	355	21	21.5
29.52505	99.39400	461819.8	3266223.6	356	24	23.5
29.52522	99.39401	461819.4	3266241.9	357	25	22.5
29.52540	99.39404	461816.1	3266262.4	357	24.5	25
29.52558	99.39407	461813.7	3266282.4	358	23	21
29.52575	99.39409	461811.4	3266300.7	360	17	14
29.52592	99.39414	461806.6	3266320.1	361	14.5	18
29.52610	99.39420	461801.3	3266339.5	361	13.5	17

29.52627	99.39427	461794.6	3266358.3	360	14	16
29.52644	99.39433	461788.4	3266377.2	360	14	16
29.52661	99.39442	461780.2	3266396.6	360	15	16
29.52677	99.39452	461770.6	3266414.4	360	15	14.5
29.52689	99.39457	461765.8	3266427.1	359	15	16.5
29.52704	99.39467	461755.6	3266444.3	361	15	14.5
29.52723	99.39485	461738.3	3266465.5	362	14	18
29.52741	99.39496	461728.2	3266485.4	361	14.5	20
29.52757	99.39506	461718.5	3266502.6	361	16	22
29.52772	99.39518	461707.0	3266519.3	362	18	21.5
29.52788	99.39525	461700.2	3266537.1	361	20	22.5
29.52801	99.39534	461691.6	3266551.5	361	21	22.5
29.52815	99.39545	461681.0	3266567.0	363	19.5	23

Line 3

Acquired May 20, 2003

20 m coil separation; 1600 Hz primary frequency

Latitude (° north)	Longitude (° west)	Easting (m)	Northing (m)	Elevation (m)	HD app. cond. (mS/m)	VD app. cond. (mS/m)
29.51213	99.39615	461607.1	3264792.2	356	4	3.5
29.51203	99.39597	461624.5	3264781.1	357	6.2	3.9
29.51191	99.39582	461638.5	3264767.7	358	7.1	1.8
29.51179	99.39568	461652.0	3264755.0	358	3.9	4.4
29.51169	99.39551	461668.9	3264743.8	358	5	4.9
29.51161	99.39533	461686.3	3264734.3	358	4.7	5.7
29.51155	99.39515	461703.8	3264727.6	359	6.3	5.2
29.51150	99.39497	461721.2	3264722.0	360	4.5	0.4
29.51145	99.39476	461741.5	3264716.4	359	7	6.5
29.51138	99.39455	461761.4	3264708.6	359	6	1.5
29.51130	99.39438	461778.3	3264699.7	360	6.2	6.1
29.51122	99.39419	461796.2	3264691.3	360	5.8	7.5
29.51111	99.39401	461813.6	3264678.5	359	6.2	7.2
29.51101	99.39384	461830.5	3264667.4	359	8.2	6.1
29.51095	99.39367	461847.0	3264660.7	360	6.9	8
29.51087	99.39350	461863.4	3264652.3	360	6.8	8.2
29.51080	99.39333	461879.9	3264644.5	360	8.7	7.7
29.51073	99.39315	461896.8	3264636.7	359	11.5	7.5
29.51061	99.39299	461912.3	3264623.3	359	18.5	4.5
29.51048	99.39284	461926.8	3264608.9	360	15.5	6.5
29.51039	99.39267	461943.2	3264598.8	359	13	11
29.51032	99.39248	461962.1	3264591.0	359	7.6	
29.51024	99.39228	461981.0	3264581.5	360	7.1	11
29.51014	99.39211	461997.4	3264571.0	360	7.1	3.5
29.51003	99.39196	462011.9	3264558.7	360	6.1	4.5
29.50991	99.39183	462024.9	3264544.8	361	5.5	4.6
29.50984	99.39162	462044.8	3264537.0	363	6.8	4.7
29.50976	99.39142	462064.6	3264528.1	363	7.9	2.3
29.50962	99.39127	462078.6	3264512.5	362	8.8	5.3
29.50948	99.39113	462092.6	3264497.5	361	11	
29.50938	99.39095	462110.0	3264486.4	361	11.5	5.5
29.50930	99.39075	462128.9	3264477.4	361	10	4
29.50917	99.39060	462143.9	3264463.0	362	7.7	5

29.50904	99.39047	462156.4	3264448.0	362	8.6	
29.50890	99.39036	462166.5	3264433.0	362	8.6	8
29.50880	99.39021	462181.0	3264421.9	362	8.7	6.5
29.50873	99.39003	462198.5	3264414.1	362	9	0.8
29.50862	99.38988	462213.4	3264401.3	362	6.2	12
29.50854	99.38967	462233.3	3264392.9	361	8	
29.50845	99.38948	462252.1	3264382.9	360	8.4	7.9
29.50829	99.38936	462263.2	3264364.5	360	6.2	14
29.50813	99.38925	462273.8	3264347.3	360	7.5	6.8
29.50796	99.38917	462282.0	3264327.9	361	15	3
29.50782	99.38910	462288.7	3264312.9	361	18	2
29.50770	99.38905	462293.1	3264299.1	361	15	
29.50751	99.38903	462295.4	3264278.6	360	8	10
29.50733	99.38898	462300.2	3264258.6	360	5.5	5.5
29.50716	99.38903	462294.8	3264239.2	361	4	4.3
29.50698	99.38913	462285.5	3264219.9	361	3.2	6.4
29.50682	99.38916	462282.1	3264201.6	361	4.2	6.2
29.50664	99.38919	462279.6	3264182.2	361	5	4.5
29.50645	99.38917	462281.0	3264161.2	361	7.4	5.2

Line 4

Acquired May 21, 2003

20 m coil separation; 1600 Hz primary frequency

Latitude (° north)	Longitude (° west)	Easting (m)	Northing (m)	Elevation (m)	HD app. cond. (mS/m)	VD app. cond. (mS/m)
29.49298	99.38995	462200.8	3262668.9	357	26	25.5
29.49314	99.39006	462190.2	3262686.7	357	25.5	34
29.49329	99.39013	462183.0	3262703.3	358	20.5	33
29.49344	99.39020	462176.3	3262719.4	359	15	28
29.49361	99.39028	462169.1	3262738.3	360	13.5	21.5
29.49379	99.39035	462161.9	3262758.2	361	15.5	23
29.49398	99.39038	462159.1	3262779.3	361	16	20.5
29.49416	99.39041	462156.7	3262799.3	361	15	21
29.49431	99.39049	462148.5	3262816.5	362	16	19.5
29.49447	99.39057	462140.8	3262834.2	363	14	17.5
29.49464	99.39064	462134.1	3262853.1	363	14	21
29.49480	99.39071	462127.9	3262870.8	363	16	21
29.49496	99.39078	462121.1	3262888.0	363	20.5	19.5
29.49516	99.39085	462114.4	3262910.8	361	35	21
29.49536	99.39091	462108.7	3262932.9	360	45	49
29.49553	99.39097	462102.9	3262951.8	359	50	40
29.49571	99.39100	462099.6	3262971.7	359	47	36
29.49589	99.39105	462095.3	3262991.1	359	38	47
29.49605	99.39112	462088.6	3263009.5	358	31	43
29.49624	99.39117	462083.8	3263030.0	357	27	31
29.49643	99.39120	462080.5	3263051.6	357	22	29
29.49659	99.39124	462076.7	3263068.8	357	18	24
29.49676	99.39129	462071.9	3263087.6	356	16	23.5
29.49693	99.39135	462066.6	3263107.0	357	17	18
29.49710	99.39139	462062.3	3263125.3	357	17	18
29.49729	99.39142	462060.0	3263146.9	357	17.5	13.5
29.49748	99.39143	462059.1	3263168.0	357	16.5	16.5

29.49766	99.39143	462059.1	3263187.9	356	18	19.5
29.49784	99.39143	462059.2	3263207.3	357	22.5	24.5
29.49801	99.39143	462059.3	3263226.2	357	26.5	40
29.49819	99.39142	462060.3	3263246.7	357	33	34
29.49838	99.39140	462062.3	3263267.2	357	38	42
29.49855	99.39137	462065.3	3263286.0	357	38	36
29.49872	99.39130	462072.1	3263304.8	357	34	32
29.49888	99.39119	462082.4	3263322.5	357	26	29
29.49903	99.39109	462092.6	3263339.1	357	18	16
29.49918	99.39100	462101.4	3263356.2	357	16	18
29.49936	99.39090	462110.6	3263375.6	356	15	10.5
29.49952	99.39082	462118.9	3263393.8	355	12.5	9.5
29.49967	99.39076	462124.3	3263409.9	355	9.5	7.8
29.49982	99.39070	462130.7	3263427.0	356	9	10.5
29.49999	99.39063	462137.5	3263445.8	356	8.7	2.3
29.50018	99.39057	462143.4	3263466.9	356	8.2	7.6
29.50035	99.39050	462149.8	3263485.7	356	8	7.2
29.50051	99.39043	462156.6	3263503.4	355	8.9	5.2
29.50068	99.39037	462162.5	3263521.7	355	9	5.8
29.50084	99.39031	462168.4	3263539.4	355	8.4	6.8
29.50100	99.39024	462175.2	3263557.6	354	7.1	6.4
29.50117	99.39018	462181.6	3263576.4	354	7	7.4
29.50136	99.39013	462186.5	3263596.9	354	7.6	8.4
29.50153	99.39007	462191.9	3263615.7	355	4.7	4.2
29.50169	99.39000	462199.2	3263633.5	355	4.8	6.4
29.50187	99.38990	462208.5	3263653.4	355	3.8	7.5
29.50205	99.38984	462214.9	3263673.3	355	4.1	6.3
29.50220	99.38980	462218.8	3263689.9	355	4.9	4.8
29.50238	99.38974	462224.7	3263710.4	354	7.5	2.1
29.50255	99.38966	462232.0	3263729.2	354	7.9	1.4
29.50268	99.38961	462236.9	3263743.6	353	4.5	1.1
29.50284	99.38954	462243.8	3263761.3	352	3.1	2.9
29.50302	99.38947	462251.1	3263780.6	351	3.8	2.8
29.50320	99.38943	462255.0	3263800.6	350	2.9	1.3
29.50337	99.38941	462257.0	3263820.0	350	2.9	4.1
29.50355	99.38938	462260.0	3263839.3	350	4.1	2.9
29.50372	99.38932	462265.4	3263858.7	349	3.5	2.6
29.50390	99.38930	462267.9	3263878.6	349	2.7	3
29.50408	99.38928	462269.9	3263898.6	350	3	2.9
29.50426	99.38924	462273.9	3263918.5	351	3.2	3.5
29.50444	99.38919	462278.8	3263937.9	351	3	3.1
29.50461	99.38916	462281.3	3263956.7	351	3.5	2.8
29.50479	99.38915	462282.3	3263976.7	352	4.9	1.5
29.50497	99.38914	462283.8	3263997.2	351	2.1	4.1
29.50515	99.38913	462284.8	3264016.5	350	4.3	5.5
29.50533	99.38912	462285.4	3264037.0	350	4.8	2.7
29.50551	99.38915	462283.0	3264057.0	349	1.8	2.5
29.50569	99.38918	462279.7	3264076.9	349	3.8	3.8
29.50587	99.38919	462279.3	3264096.9	349	4	5.1
29.50604	99.38918	462279.8	3264115.7	348	4	2.8
29.50623	99.38918	462280.4	3264136.8	349	5.1	3.8
29.50641	99.38918	462280.5	3264156.7	350	5.5	4.5

Line 5

Acquired May 21, 2003

20 m coil separation; 1600 Hz primary frequency

Latitude (° north)	Longitude (° west)	Easting (m)	Northing (m)	Elevation (m)	HD app. cond. (mS/m)	VD app. cond. (mS/m)
29.48383	99.35558	465529.4	3261644.4	340	20.5	16
29.48400	99.35549	465537.7	3261662.7	341	19	9
29.48417	99.35542	465545.0	3261681.5	341	17	12
29.48432	99.35534	465552.8	3261698.6	341	15	14
29.48448	99.35526	465560.7	3261716.3	341	14.5	12.5
29.48464	99.35516	465570.4	3261734.0	341	16	14
29.48481	99.35505	465580.6	3261752.3	341	16.5	9
29.48496	99.35495	465590.9	3261769.4	341	11.5	9
29.48511	99.35485	465600.1	3261785.5	341	10.5	9.5
29.48528	99.35476	465608.9	3261804.8	341	8.5	6.5
29.48546	99.35467	465618.2	3261824.2	341	7.5	5
29.48563	99.35459	465626.0	3261843.0	342	5.2	5.3
29.48578	99.35446	465638.6	3261859.6	343	4.6	3.5
29.48588	99.35430	465654.2	3261870.6	344	5.6	4.3
29.48600	99.35416	465667.3	3261883.9	344	4.1	3.4
29.48615	99.35406	465677.6	3261901.0	343	6.3	3.6
29.48630	99.35396	465687.3	3261917.1	343	5.5	2
29.48647	99.35386	465697.0	3261936.4	343	4.7	4.3
29.48664	99.35376	465706.8	3261955.2	342	4.3	3.3
29.48678	99.35365	465717.5	3261970.2	341	3.2	1.2
29.48691	99.35355	465726.8	3261985.1	341	2.5	3.9
29.48706	99.35341	465740.4	3262001.7	340	2.5	5.3
29.48718	99.35323	465758.4	3262014.9	340	3.1	3.2

Line 6

Acquired May 21, 2003

20 m coil separation; 1600 Hz primary frequency

Latitude (° north)	Longitude (° west)	Easting (m)	Northing (m)	Elevation (m)	HD app. cond. (mS/m)	VD app. cond. (mS/m)
29.48329	99.35601	465487.1	3261584.2	339	42	26
29.48323	99.35621	465467.7	3261577.6	340	39	25
29.48318	99.35638	465451.6	3261572.6	340	36	39
29.48310	99.35654	465435.6	3261563.8	340	40	30
29.48298	99.35669	465421.5	3261550.0	340	47	33
29.48280	99.35678	465412.2	3261530.6	340	53	39
29.48261	99.35684	465406.9	3261509.6	340	59	38
29.48243	99.35686	465404.9	3261489.1	341	55	39
29.48225	99.35690	465400.9	3261469.7	340	49	44
29.48211	99.35698	465393.1	3261453.7	340	43	53
29.48198	99.35708	465382.9	3261439.3	340	39	46
29.48184	99.35722	465369.3	3261423.9	340	38	41
29.48170	99.35738	465354.2	3261408.4	340	39	39
29.48159	99.35755	465337.7	3261396.8	340	39	43
29.48151	99.35775	465318.3	3261388.0	339	39	49
29.48145	99.35794	465299.3	3261380.9	339	39	44
29.48143	99.35810	465284.3	3261379.2	339	41	42
29.48140	99.35829	465265.4	3261375.4	339	42	39

29.48134	99.35852	465243.1	3261368.8	339	43	41
29.48131	99.35873	465222.7	3261366.1	338	48	43

Line 7

Acquired May 22, 2003

20 m coil separation; 1600 Hz primary frequency

Latitude (° north)	Longitude (° west)	Easting (m)	Northing (m)	Elevation (m)	HD app. cond. (mS/m)	VD app. cond. (mS/m)
29.50252	99.34682	466384.3	3263712.2	354	3	2.1
29.50270	99.34684	466382.4	3263732.1	354	2.8	1.5
29.50287	99.34688	466378.6	3263751.0	354	2.6	2
29.50304	99.34694	466373.4	3263770.4	355	2.8	2.4
29.50322	99.34701	466366.6	3263789.8	355	3.1	1.4
29.50338	99.34709	466358.4	3263807.5	355	3	1.9
29.50352	99.34721	466346.9	3263823.6	355	2.7	2.2
29.50364	99.34736	466332.4	3263837.0	355	2.8	2.8
29.50376	99.34753	466316.4	3263849.8	356	2	1.5
29.50389	99.34768	466301.9	3263864.8	358	3.5	1.5
29.50404	99.34776	466294.2	3263881.4	359	3.8	2.6
29.50421	99.34773	466296.7	3263899.7	359	4.4	1
29.50437	99.34764	466305.9	3263917.4	358	6.5	5.2
29.50453	99.34754	466315.2	3263935.6	357		2.1
29.50469	99.34755	466314.8	3263953.4	358	4.8	5
29.50480	99.34772	466297.9	3263965.6	359	2.9	3.2
29.50490	99.34793	466278.0	3263976.2	360	2.4	4.1
29.50503	99.34805	466266.4	3263991.2	362	2.6	3.1
29.50519	99.34814	466257.3	3264008.9	363	3.3	1.1
29.50537	99.34823	466248.6	3264028.4	364	1.9	2.4
29.50553	99.34828	466244.3	3264046.7	365	1.5	2.1

Line 8a

Acquired May 22, 2003

10 m coil separation; 6400 Hz primary frequency

Latitude (° north)	Longitude (° west)	Easting (m)	Northing (m)	Elevation (m)	HD app. cond. (mS/m)	VD app. cond. (mS/m)
29.47808	99.34634	466423.3	3261004.6	341	24	28
29.47800	99.34634	466422.8	3260995.2	341	23.5	26
29.47791	99.34635	466421.8	3260985.8	341	24	25
29.47781	99.34635	466421.7	3260974.1	341	24.5	26
29.47770	99.34636	466421.2	3260962.5	340	25	25
29.47761	99.34636	466420.7	3260952.0	340	25	31
29.47752	99.34636	466420.7	3260942.0	340	30	35
29.47743	99.34637	466420.2	3260932.6	339	39	28
29.47735	99.34637	466419.6	3260923.7	340	53	32
29.47726	99.34637	466419.6	3260913.2	340	61	44
29.47716	99.34639	466418.1	3260902.1	340	69	46
29.47707	99.34641	466415.7	3260892.2	340	72	51

Line 8b

Acquired May 22, 2003

20 m coil separation; 1600 Hz primary frequency

Latitude (° north)	Longitude (° west)	Easting (m)	Northing (m)	Elevation (m)	HD app. cond. (mS/m)	VD app. cond. (mS/m)
29.47805	99.34635	466422.3	3261000.7	341	32	35
29.47795	99.34634	466422.8	3260989.7	341	32	29
29.47786	99.34635	466421.8	3260979.7	340	33	33
29.47776	99.34636	466421.2	3260968.6	341	33	35
29.47766	99.34636	466421.2	3260957.5	340	35	33
29.47756	99.34636	466420.7	3260947.0	340	37	43
29.47748	99.34637	466420.2	3260937.6	340	42	44
29.47739	99.34637	466420.1	3260928.2	340	49	35
29.47730	99.34637	466419.6	3260917.6	340	56	34
29.47721	99.34639	466418.1	3260908.2	340	66	37
29.47711	99.34640	466417.1	3260897.2	340	70	35

Line 8c

Acquired May 22, 2003

40 m coil separation; 400 Hz primary frequency

Latitude (° north)	Longitude (° west)	Easting (m)	Northing (m)	Elevation (m)	HD app. cond. (mS/m)	VD app. cond. (mS/m)
29.47794	99.34635	466422.3	3260989.1	341	32	34
29.47784	99.34635	466422.2	3260978.0	341	33	28
29.47776	99.34636	466421.2	3260969.2	340	34	29
29.47767	99.34636	466421.2	3260958.6	340	37	36
29.47757	99.34636	466420.7	3260948.1	340	39	34
29.47748	99.34637	466420.2	3260938.1	340	42	31
29.47738	99.34637	466420.1	3260927.1	340	45	29
29.47729	99.34638	466418.7	3260917.1	340	50	21
29.47721	99.34640	466417.2	3260907.7	340	53	16

Line 9a

Acquired May 22, 2003

10 m coil separation; 6400 Hz primary frequency

Latitude (° north)	Longitude (° west)	Easting (m)	Northing (m)	Elevation (m)	HD app. cond. (mS/m)	VD app. cond. (mS/m)
29.48325	99.36108	464996.0	3261581.8	346	14	23
29.48333	99.36105	464998.5	3261590.6	345	14	23
29.48342	99.36104	465000.0	3261600.6	345	16	14.5
29.48352	99.36103	465001.0	3261611.7	345	17	20.5
29.48360	99.36101	465002.9	3261620.6	345	16	21.5
29.48369	99.36098	465005.9	3261630.0	344	15	19.5
29.48378	99.36096	465007.8	3261639.9	344	16.5	20
29.48388	99.36094	465009.8	3261651.0	344	19	17
29.48397	99.36093	465010.8	3261661.5	345	18.5	18
29.48405	99.36091	465012.3	3261670.4	344	17	19.5
29.48414	99.36089	465014.3	3261679.8	344	13.5	13.5
29.48422	99.36087	465016.2	3261688.7	345	11.5	18
29.48431	99.36086	465017.7	3261698.6	346	11	15.5
29.48441	99.36085	465018.2	3261709.7	348	11	16

29.48450	99.36082	465021.7	3261719.7	348	11	16
29.48454	99.36080	465023.6	3261724.1	347	13	16.5
29.48458	99.36079	465024.1	3261728.5	347	15.5	17.5
29.48466	99.36078	465025.6	3261737.9	349	17.5	21
29.48475	99.36077	465026.6	3261747.3	349	22	17.5
29.48484	99.36075	465028.1	3261757.9	348	25	14

Line 9b

Acquired May 22, 2003

20 m coil separation; 1600 Hz primary frequency

Latitude (° north)	Longitude (° west)	Easting (m)	Northing (m)	Elevation (m)	HD app. cond. (mS/m)	VD app. cond. (mS/m)
29.48328	99.36107	464997.0	3261585.1	346	21	29
29.48339	99.36105	464999.0	3261597.3	345	20	21
29.48346	99.36103	465000.5	3261605.0	345	19.5	17.5
29.48356	99.36101	465002.4	3261616.1	345	19.5	21.5
29.48365	99.36099	465004.4	3261625.5	344	19.5	21
29.48373	99.36097	465006.4	3261634.9	344	19	20
29.48383	99.36094	465009.3	3261646.0	344	19	15.5
29.48392	99.36094	465009.3	3261655.4	345	18.5	12.5
29.48401	99.36091	465012.8	3261665.9	344	18.5	15
29.48410	99.36091	465012.3	3261675.4	345	17	13.5
29.48417	99.36087	465016.2	3261683.7	344	16	17
29.48427	99.36088	465015.8	3261694.7	346	16	17.5
29.48435	99.36085	465018.7	3261703.6	347	15.5	18
29.48445	99.36083	465020.7	3261714.7	348	15.5	18
29.48449	99.36082	465021.2	3261719.1	347	16	20
29.48458	99.36079	465024.6	3261729.1	348	17.5	19
29.48462	99.36079	465024.6	3261732.9	347	19	19.5
29.48471	99.36077	465026.1	3261742.9	348	21.5	17
29.48480	99.36076	465027.6	3261752.9	349	20.5	8

Line 9c

Acquired May 22, 2003

40 m coil separation; 400 Hz primary frequency

Latitude (° north)	Longitude (° west)	Easting (m)	Northing (m)	Elevation (m)	HD app. cond. (mS/m)	VD app. cond. (mS/m)
29.48338	99.36106	464998.0	3261596.2	346	18	15.5
29.48347	99.36103	465000.9	3261606.2	345	18	13.5
29.48355	99.36100	465003.4	3261614.5	344	17	11
29.48365	99.36099	465004.4	3261626.1	345	17	12.5
29.48375	99.36097	465006.4	3261636.6	345	16.5	11
29.48383	99.36096	465007.4	3261645.5	345	16	9
29.48391	99.36093	465010.8	3261654.9	343	14.5	7.5
29.48400	99.36092	465011.3	3261664.8	345	14.5	7
29.48409	99.36089	465014.7	3261674.8	345	15	9
29.48419	99.36090	465013.8	3261685.3	346	15.5	9
29.48427	99.36087	465016.7	3261694.7	346	15	12
29.48436	99.36084	465019.2	3261704.7	347	14.5	12.5
29.48439	99.36083	465020.7	3261708.0	345	15	12
29.48449	99.36082	465021.2	3261719.1	348	15	10.5

29.48458	99.36081	465022.7	3261728.5	349	15.5	10.5
29.48467	99.36078	465025.6	3261738.5	348	17	5
29.48471	99.36077	465026.1	3261743.5	347	16	1.5